

MCMEG: Intercomparison exercise on prostate radiotherapy dose assessment



T.C.F. Fonseca^{a,b,*}, P.C.G. Antunes^e, M.C.L. Belo^c, F. Bastos^f, T.P. Campos^{a,b}, J.M. Geraldo^{d,f}, A.M. Mendes^b, B.M. Mendes^c, L. Paixão^d, P.C. Santana^d, B. Seniwal^b, P.L. Squair^c, H. Yoriyaz^e

^a Departamento de Engenharia Nuclear – DEN BH/MG, Brazil

^b Programa de Pós-graduação em Ciências e Técnicas Nucleares - UFMG BH/MG, Brazil

^c Centro de Desenvolvimento de Tecnologia Nuclear – CDTN/CNEN, BH/MG, Brazil

^d Departamento de Anatomia e Imagem, Faculdade de Medicina - UFMG BH/MG, Brazil

^e Instituto de Pesquisas Energéticas e Nucleares CNEN – SP, Brazil

^f Hospital Luxemburgo, BH/MG, Brazil

ARTICLE INFO

Keywords:

MCMEG
Monte Carlo
Radiotherapy
Intercomparison exercise
Alderson phantom
TLDs

ABSTRACT

The improvement of the Monte Carlo (MC) community skills on computational simulations in Medical Physics is crucial to the field of radiotherapy as well as radiology. The Monte Carlo Modelling Expert Group (MCMEG) is an expert network specialized in MC radiation transport modelling and simulation applied to the radiation protection and dosimetry research fields. The MCMEG addressed a multigroup dosimetric intercomparison exercise for modelling and simulating a case of prostate radiation therapy (RT) protocol. This intercomparison was launched in order to obtain the dose distribution in the prostate target volume and in the neighboring organs. Dose assessments were achieved by using TLDs. A protocol using two pair of parallel-opposed fields were planned and performed with Alderson-Rando Pelvic Phantom. The assessed organs at risk were the urinary bladder, rectum and right and left femur heads. The RT simulations were performed using the MCNPx, MCNP6 and egs++ and BEAMnrc/DOSXYZnrc modules of EGSnrc Monte Carlo codes. The dose to the target volume, mean doses and standard deviation in the organs at risk, and dose volume data were computed. A comparison between the simulated results and the experimental values obtained from TLD measurements was made. In some cases the results obtained using MC simulations showed large deviations in comparison to the results obtained from the TLD measurements and these variations can be explained by the difficulties in the modelling of the geometry, selection of MC parameters required for the simulations and the statistical errors and inaccuracies in experimental measurements. Even though, the exercise has been a great opportunity for the MC groups to learn and share the main difficulties found during the modelling and the analysis of the results. Concerned to the obtained variations, the MCMEG team consider that this was expected for the level of complexity of the exercise and must be studied by the MC groups.

1. Introduction

Radiation therapy (RT) is often used in combination with surgery and chemotherapy to improve its outcomes (Ross, 1999). Many factors involving the RT plan and the radiation delivery procedures must be considered in order to carry out an efficient treatment. In radiation dosimetry, quality assurance also plays important role. Various calibration tools and dosimeters are available in the market that can be used to perform quality assurance tests at different accuracy levels. Thermoluminescent dosimeters (TLDs) are used for measurements in radiation therapy, mostly for studies including anthropomorphic

phantoms, *in vivo* dosimetry on patients, and surface dose measurements (Budanec et al., 2008; Gardner et al., 2012; Tai et al., 2017). Moreover, the application of TLDs has been suggested in the case of radiopharmaceutical nanoagents (Seemann et al., 2015). Thermoluminescent dosimetry is a well established technique used for several applications in radiotherapy, as an example, it can be used in clinical dosimetry. LiF:Mg,Ti (TLD-100) is one of the extensively used TLD for routine dosimetry due to its tissue equivalence, broad linear response (from 10 μ Gy up to 10 Gy) reasonable signal fading (5–10% per year) and high sensitivity towards low dose measurement (Chen and Leung, 2001; Montano-Garcia and Gamboa-de Buen, 2006; James D. Rijken,

* Corresponding author. Departamento de Engenharia Nuclear – DEN BH/MG, Brazil.

E-mail addresses: telmafonseca@nuclear.ufmg.br, tcff01@gmail.com (T.C.F. Fonseca).

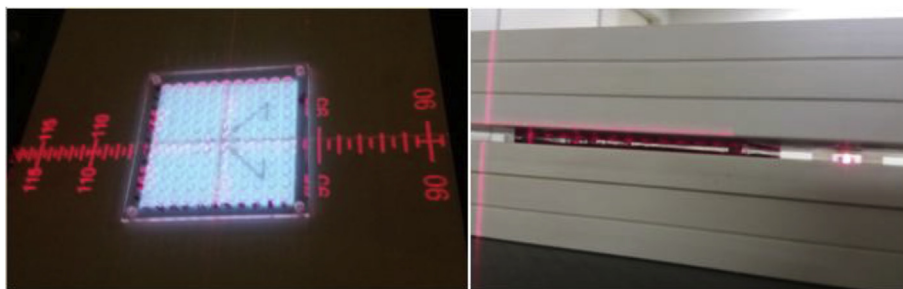


Fig. 1. Calibration set-up for LiF:Mg,Ti detectors in 6 MV beam. Left figure shows the acrylic tray with the TLDs and right side shows the arrangement of slabs above and below the acrylic tray.

2014). Also, its small size makes it a good choice for point dose measurements within the phantoms and for *in vivo dosimetry* (B.S. Limited, 2014). In addition, TLD-100 can be effectively used in both continuous and pulsed radiation beams, requiring less correction factors to measure the absorbed dose (B.S. Limited, 2014). Therefore, TLD-100 becomes an ideal dosimeter for most of the RT dosimetry.

A suitable education training on medical physics dosimetry is very important for dosimetric intercomparisons in radiation therapy embracing multigroup specialists. Several studies have been performed using Monte Carlo codes in the field of medical physics (Budaneć and Knežević, 2008; Paixão et al., 2012; Fonseca and Campos, 2016). In 2010, Schiefer et al. (2010) conducted a dosimetric intercomparison for Intensity Modulated Radiation Therapy (IMRT) on radiation therapy facilities in Switzerland. The aim of this intercomparison was to provide information about how well the radiotherapy is delivered. Authors compared TLD and ion chamber measurements with respect to the dose calculation algorithms used in the treatment planning algorithms. The authors found that, in case of low density tissue such as lung tissue, type b dose calculation (Knöös et al., 2006) algorithms are more accurate, whereas in absence of low density tissue both type a and b algorithms have similar accuracy level.

The Monte Carlo Modelling Expert Group (MCMEG) (MCMEG, 2018) is an expert network specialized in MC radiation transport modelling and simulation applied to the radiation protection and dosimetry research fields. Today, the MCMEG has 53 members from various institutes of different countries and new members are always welcome to join the group. In 2016, the group published its first inter-comparison exercise to model and simulate a 6 MV LINAC photon beam using different MC codes (Fonseca et al., 2017). The validation of the simulation was done by comparison PDD and TPR results with experimental measurements carried out in the National Cancer Institute (INCA) in Rio de Janeiro, Brazil. The intercomparison exercise demonstrated its relevance by showing the influence of different modelling approaches and different MC codes, achieving interesting analysis.

In 2017, the MCMEG launched its second intercomparison exercise for modelling and simulating a case of prostate radiotherapy protocol. This intercomparison was launched with the aim to obtain the dose distribution in the target volume and at the neighboring organs. The similar treatment plan is generated using different Monte Carlo codes, commercial treatment planning system and experimental dosimetric data assessed by using LiF:Mg,Ti TLDs. Four groups of the Brazilian territory participated in this exercise using different MC codes. The groups are from the following institutions: Instituto de Pesquisas Energéticas e Nucleares (IPEN) in São Paulo city, the Faculty of Medicine of Universidade Federal de Minas Gerais (UFMG), the Hospital Luxemburgo (HL), the Department of Nuclear Engineering of UFMG and the Centro de Desenvolvimento da Tecnologia Nuclear (CDTN) in Belo Horizonte city. Four different codes were used: MCNP6 (Werner et al., 2018; Werner, 2017), the MCNPX (Goorley et al., 2012; Pelowitz, 2011; Rogers, 2006), the EGS++ and the BEAMnrc/DOSXYZnrc/EGSnrc (Mainegra-Hing et al., 2017). This study describes an

inter-comparative analysis of the dose distributions using MC codes with the data measured with TLDs placed in the Alderson-Rando Pelvic Phantom and reports an intercomparison exercise done by different groups of researchers.

2. Material and methods

2.1. TLD dosimetry - calibration

A group of ten LiF:Mg,Ti (TLD-100) disks of diameter of 4.5, thickness of 0.89 mm and density of 2.64 g cm^{-3} were used for the calibration with respect to the 6 MV photon beam. The calibration was performed in the radiotherapy sector of the Hospital Luxemburgo in Belo Horizonte, Brazil. The TLDs were placed at the center of an acrylic tray and it was placed between 6 cm of water equivalent acrylic slabs (Bouchard and Seuntjens, 2004). Each slab had the dimensions of $30 \text{ cm} \times 30 \text{ cm} \times 1 \text{ cm}$. Three slabs were placed below the tray and the other three above the acrylic tray. The TLDs were irradiated on the linear accelerator with a 6 MV photon beam, field size $10 \times 10 \text{ cm}^2$, surface source distance (SSD) of 100 cm, with the dose of 0.8 Gy similar to the dose used for the irradiation of the Alderson-Rando Pelvic Phantom. Fig. 1 shows the experimental set-up used for the calibration of the TLDs.

3. Experimental procedure

The experiments were performed in the Radiotherapy Center of the Hospital Luxemburgo (HL). LiF:Mg,Ti thermoluminescent dosimeters (TLDs) were placed in the physical phantom at reference points of the Alderson-Rando Pelvic Phantom region covering all the organs of interest (ROIs): the urinary bladder, rectum, femur heads (right and left), extremities as well as target volume, the prostate. Fig. 2 shows a sketchup of the TLD placement points on a Alderson-Rando slice.

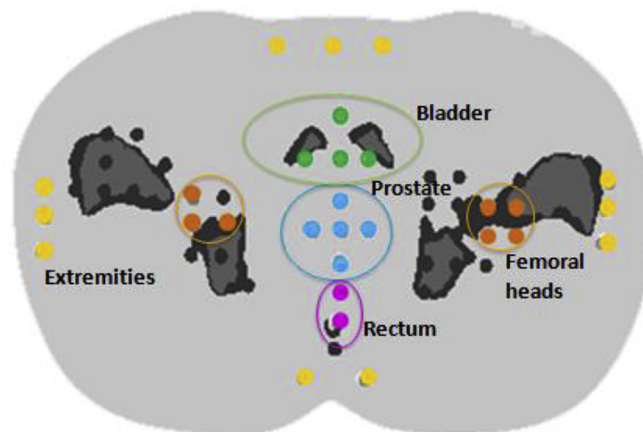


Fig. 2. Sketchup of the TLD placement points on a Alderson slice.

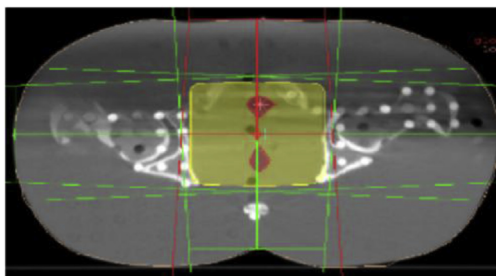


Fig. 3. The positioning of four fields on the CT slice of Alderson-Rando Pelvic Phantom using Xio Treatment Planning System and the dose distribution is shown in yellow. (For interpretation of the references to each organ, the reader is referred to the Web version of this article.)

CT scan of the Alderson-Rando Pelvic Phantom with the TLDs placed within the cavities was obtained and the DICOM images were used for the MC modelling and simulation. The CT scan was performed in a Siemens Tomograph scanner, Somatom model, with the exposure factors of 130 kV and 70 mAs, corresponding to a pelvic tomography routine settings. A slice thickness of 2 mm was used. The phantom was placed in dorsal decubitus position with the laser focused between the midline at the slices of number 32 and 33 of the phantom.

3.1. Irradiation of the Alderson-Rando Pelvic Phantom

The **Alderson-Rando phantom** was irradiated with a 6 MV photon beam from the linear accelerator, Elekta Precise. Four-field parallel-opposed treatment plan was set using the XiO treatment planning system (TPS) prescribing a total of 0.8 Gy to the target volume, prostate. The TPS used superposition dose calculation algorithm. The isocentric treatment plan was established with four-orthogonal radiation portals with gantry orientation of 0, 90, 180, 270°, 10 × 10 cm² field size and a source to axis distance (SAD) of 100 cm. Fig. 3 shows the positioning of the four-portals on a CT slice of the Alderson-Rando Pelvic Phantom and the dose distribution depicted in yellow color, provided by the XiO TPS. The experimental setup was similar according to the proposed TPS plan. The standard deviation of the TLDs measurement is 0,15 Gy.

4. Computational modelling

Four groups from different institutions participated in this inter-comparison exercise. The MCNPx, MCNP6, EGSnrc (egs++ and BEAMnrc/DOSXYZnrc) Monte Carlo codes were used to calculate the dose distribution in the voxelized Alderson-Rando Pelvic Phantom. Each group was free to develop their own model and simulation. All the necessary information was provided to the groups such as, the DICOM images and the voxelized phantom, the material composition of the phantom and the spectrum of the radiation source.

The voxelized phantom was developed from the CT images of the Alderson-Rando Pelvic Phantom pelvic region with the help of semi-automatic segmentation process with ImageJ[®] software (Xu and Eckerman, 2010). As CT images generally show resolutions higher than necessary for the simulations, ImageJ[®] was used to reduce the resolution of the images (Mendes et al., 2014). The voxelized Alderson-Rando Pelvic Phantom had matrix dimension of 366 × 244 × 113 and 0.96 × 0.96 × 2.0 cm³ voxel dimensions. The segmented voxelized phantom had different ID numbers for each TLD belonging to the organs at risk and target volume. ID number were also provided for media such as air, bones and soft tissue. The number of TLDs placed in each of the ROI was, 6 in prostate, 9 in bladder, 8 in rectum, 5 in right femur, 6 in left femur, 3 in anterior extremities, 2 in posterior extremities, 3 in left extremities and 3 TLDs were placed in right extremities. Table 1 shows the serial number of TLDs and their respective organs. The TLDs

Table 1
TLDs correspondent ID to each organ.

Organs	TLD-ID
Prostate	22, 23, 24, 25, 26, 33
Bladder	3, 4, 5, 6, 11, 12, 13, 14, 15
Rectum	1, 2, 9, 10, 20, 21, 31, 32
Right Femur Head	7, 8, 18, 19, 30
Left Femur Head	16, 17, 27, 28, 29, 34
Extremity anterior	40, 41, 42
Extremity left	43, 44, 45
Extremity right	35, 36, 37
Extremity posterior	38, 39

Table 2
Weight fractions of the elemental composition of LiF:Ti,Mg (Abushab et al., 2017).

Element	Weight fractions
Lithium	0.2672
Fluorine	0.7328
Magnesium	0.0002
Titanium	0.00001

position were segmented in the voxelized phantom using different ID numbers and sent by the organizers to the MC groups. The elemental composition of the TLDs used in the modelling are shown in Table 2.

All the groups agreed to model radiation source as a point source emitting 6 MV photon beam spectrum provided by the organizers and published in the previous MCMEG exercise (Fonseca et al., 2017). For the material compositions of the air, bones and soft tissue each MC group was free to set the material composition according to their convenience.

4.1. Group 1

G1 used the MCNP6.11 version of MC code. They used the voxelized phantom. The 6 MV spectrum provided by the organizers was used to configure the radiation as source placed at a distance of 100 cm from the isocenter. The isocenter of the phantom was set in relation to the photon beam at the following coordinates 17.568 × 11.712 × 11.2 cm.

A command provide by MCNP code is the direction command (DIR) and it was set as 0.9987523, providing a field size of 10 × 10 cm² at the isocenter of the phantom. Four input files were developed to set the different directions of the radiation source being 0°, 90°, 180° and 270°. Mode card was set as p, e which take care of the transport of photons and electron produced in the model. In all simulations, the cross section library used was set to photons as MCPLIB 84 and for electrons the el032. The energy cut off was set as 10 keV and the electrons up to 100 keV.

For the scoring of the absorbed dose in the voxel: *F8, F6 + FM (FM to correct the mass of the voxel) and *F4 + DE/DF which uses the mass coefficient of absorption energy of the TLD LiF, tallies were utilized. The number of particles was set as 1E10, in order to reduce the relative error. This group used a cluster Silicon Graphics Altix XE 340 with 121 processors and each input file took about 4 h for running. The material composition as air, soft tissue, adult bone Alderson, bone cortical and the TLD were found in ATOM phantoms (Computerized Imaging Reference Systems, Inc, Norfolk, VA) and Shen et al. (2018); I.C.R.U., 1992.

4.2. Group 2

G2 used MCNPx code and the voxelized Alderson-Rando Pelvic Phantom provide by the organizers. A collimated 6 MV photon beam was set as a radiation source at 100 cm from the isocenter of the

phantom considering the prostate of the phantom as origin. The spectrum provided by the organizers was used and the collimator jaws were added in the computational model. The cone photon source was positioned above the collimator jaws, in such way that the radiation field size was slightly higher than the square opening of the collimator jaws. The cone source was configured as Castelo e Silva, et. al. 2016 (Castelo e Silva et al., 2016). A $10 \times 10\text{cm}^2$ field size was obtained at the isocenter of the phantom as requested in the inter-comparison exercise. Four different input files were developed in order to obtain the different directions of the radiation source, 0° , 90° , 180° and 270° . The + F6 tally card of MCNPx was used to score the dose in MeV per gram per particle of each TLD separately. The results of each output file provide by the MC code after simulation was used to sum and the total normalized dose in each TLD was obtained. TLDs were then added together to obtain doses in each organ separately. Assuming that 0.8Gy dose was received by the TLDs of the prostate the dose deposited inside other organs of interest was calculated. The simulations were done in the high-performance cluster for computational calculations of the IRD/CNEN laboratory Orion. The number of particles was set as $1\text{E}8$ in order to have relative error below 3% and the time of the simulation for each input has around 40 min.

4.3. Group 3

G3 used EGSnrc (EGS++) code (Kawrakow et al., 2009). This group also used the voxelized phantom and the spectrum provided by the organizers of this intercomparison. They used the EGSnrc materials library for the composition of the air, soft tissue, bone and cortical bone. A point source was modeled emitting a 6 MV photon beam spectrum. The X-ray beam was collimated to a $10 \times 10\text{cm}^2$ dose scoring field positioned at the isocenter with a distance of 100 cm from the source. Four radiation fields were considered to simulate the four-field LINAC gantry treatment positions: 0° , 90° , 180° and 270° . The input files were written according to the EGSnrc C++ class library geometric package. The *tutor7pp* user-code was used in the simulations to score medium dose through an *ausgab* object. The Monte Carlo transport parameters selected for the electron and photon transport were 10 keV cutoff energy, XCOM photon and Compton cross sections, NIST Bremsstrahlung cross-sections and simple mode set for bound Compton scattering. All other EGSnrc MC transport parameters were kept at the default values. No variance reduction options were selected. $5\text{E}8$ particles were simulated to obtain a relative error of 1% or less on calculated quantities. The simulations were performed on a computer with eight Intel® Core™ i7 of 3.40 GHz and 8 GB RAM. The time of the simulation of one input file with the four field together was about 6 h.

4.4. Group 4

G4 used BEAMnrc/DOSXYZnrc (EGSnrc, 2017). The simulation was done in three steps, firstly modelling the voxelized CT phantom for DOSXYZnrc using CTCREATE (Walters et al., 2005) module of EGSnrc.

Linear relationship between the mass density and CT numbers of the materials was developed to obtain the voxelized phantom in a similar manner as done by Seniwal et al., (2019) (Seniwal et al., 2019). The material composition of soft tissue and adult bone were obtained from ATOM phantoms (Computerized Imaging Reference Systems, Inc, Norfolk, VA) this provided different ID numbers to different media namely air, soft tissue, bone and TLDs. Secondly, point source emitting 6 MV photon beam spectrum provided by the organizers was modeled and source was placed 27.5 cm above the jaws in such a way that $10 \times 10\text{cm}^2$ field size was obtained at isocenter, at a distance of 100 cm from the source. Phase space file for $10 \times 10\text{cm}^2$ was obtained using BEAMnrc (Rogers et al., 2009; Kawrakow et al., 2004) (EGSnrc, 2017) with dose scoring below the LINAC jaws. Lastly, the phase space file and voxelized phantom file were used as input in DOSXYZnrc (Walters et al., 2005) and dose calculation was done for all four radiation fields using isocentric techniques with source to axis distance (SAD) of 100 cm one by one. Directional Bremsstrahlung Splitting was used as a variance reduction technique with a splitting number of 1000 and radius of 10 cm (Kawrakow et al., 2004). Physics parameters were taken from Kawrakow et al. (Kawrakow, 2000) and the values for ECUT = AE = 0.7 MeV and PCUT = AP = 0.01 MeV were used. The Particle Transport and EGS parameters ECUTIN, PCUTIN, ESAVE_GLOBAL and IREJECT_GLOBAL were implemented into the program to reduce the simulation time by eliminating those particles that have less significant contribution to the dose in the region of interest (Pham, 2009). $7\text{E}8$ particles were simulated to obtain the relative error of less than 1%. The simulations were performed using computer with eight Intel® Core™ i5 of 3.40 GHz and 8 GB RAM. The *3ddose* files were obtained at the end of simulation and these files were nothing but 3 dimensional dose matrix containing information about dose distribution, in terms of dose per incident particle say, Gy per number of events, inside the voxels of the phantom. Finally, the *3ddose* data files were imported into CERR, the Computational Environment for Radiotherapy Research software for analysis and dose to each TLD was obtained as the sum of doses received from each radiation field. The time of about ~4 h taken to simulate the dose deposited by each radiation.

5. Results and discussion

The organizers of the MCMEG requested to the participating MC groups to submit their results of the intercomparison exercise in terms of (1) the total absorbed dose in each TLD as well as in (2) the dose deposited within the organs. The TLDs were placed at reference points in the Alderson-Rando Pelvic Phantom region covering all the organs of interest (ROIs) say, the urinary bladder, rectum and femur (right and left) and the target organ, prostate. Thus, in order to have the total dose per organ, the MC groups have to have all the ID of the TLDs as shown in Table 1. For instance, to calculate the total dose in the organ, it was used the scoring data provided by the + F6 tally card of MCNPx in MeV per gram per particle of each TLD separately, afterwards, the TLDs doses were summed to have doses in each organ separately. Assuming,

Table 3
Dosimetry in prostate and organs at interest, for the Monte Carlo codes, and experimental measurements by TLDs.

Organs	Prostate	Bladder	Rectum	Left Femur	Right Femur	Anterior Extremities	Posterior Extremities	Left Extremities	Right Extremities
TLD (Gy)	0.8	0.7	0.62	0.46	0.47	0.48	0.47	0.54	0.55
G 1 (MCNP6 (Gy))	0.8	0.69	0.58	0.40	0.37	0.53	0.54	0.49	0.51
**Δ (%) TLD		1.0	6.0	13.0	21.0	-10.0	-15.0	9.0	7.0
G 2 (MCNPx)	0.8	0.64	0.74	0.53	0.64	0.67	0.46	0.47	0.66
**Δ (%) TLD		9.0	-19.0	-15.0	-36.0	-40.0	-2.0	13.0	-20.0
G3 EGSnrc (EGS++)	0.8	0.67	0.67	0.41	0.39	0.52	0.52	0.47	0.49
**Δ (%) TLD		4.0	-8.0	11.0	17.0	-8.0	-11.0	13.0	11.0
G4 EGSnrc (BEAMnrc/DOSXYZnrc)	0.8	0.75	0.65	0.41	0.41	0.52	0.51	0.44	0.44
**Δ (%) TLD		-7.0	-5.0	11.0	12.0	-8.0	-10.0	19.0	19.0

*Δ (%) TLD percentage variation with respect to TLD dosimetry.

Table 4

The doses obtained for each of the 45 TLDs and percentage variations obtained for each TLD doses and for all MC groups.

TLD ID	1	2	3	4	5	6	7	8	9	10	11
Organ**	R	R	B	B	B	B	LF	LF	R	R	B
I/O/E*	I	I	I	I	O	E	O	O	I	I	I
TLD Dose (Gy)	0.7	0.8	0.7	0.7	0.5	0.5	0.5	0.5	0.5	0.8	0.8
G1 Δ(%) TLD	30.6	-0.7	24.2	23.0	-9.4	-25.3	14.4	12.5	-6.5	4.5	-9.2
G2 Δ(%) TLD	-0.4	17.4	17.5	10.0	42.4	-43.9	-28.9	-27.2	-53.8	0.7	-4.3
G4 Δ(%) TLD	-15.4	-6.4	-4.9	-10.0	-2.9	-75.2	13.3	11.3	-50.1	-0.2	-1.0
TLD ID	12	13	14	15	16	17	18	19	20	21	22
Organ**	B	B	B	B	RF	RF	LF	LF	R	R	P
I/O/E*	I	I	I	I	O	E	O	O	I	I	I
TLD Dose (Gy)	0.8	0.8	0.7	0.8	0.5	0.4	0.5	0.5	0.5	0.8	0.8
G1 Δ(%) TLD	4.5	-4.0	-18.0	-8.0	10.9	10.2	11.5	10.9	-3.9	23.7	-1.9
G2 Δ(%) TLD	6.4	-0.5	-7.3	-3.5	-62.5	-70.6	0.5	0.2	-45.3	-5.2	0.0
G4 Δ(%) TLD	6.4	3.5	-10.9	-2.1	10.7	9.7	11.2	9.2	-39.9	-5.0	1.1
TLD ID	23	24	25	26	27	28	29	30	31	32	33
Organ**	P	P	P	P	RF	RF	RF	RF	R	R	R
I/O/E*	I	I	I	I	E	E	O	O	O	E	I
TLD Dose (Gy)	0.8	0.8	0.8	0.8	0.5	0.5	0.5	0.5	0.5	0.5	0.8
G1 Δ(%) TLD	-2.5	1.2	2.8	0.4	17.2	18.9	17.2	31.1	-7.5	-7.7	8.7
G2 Δ(%) TLD	-1.1	1.2	2.8	1.8	-60.8	-60.9	9.6	22.7	-37.5	-60.9	-1.6
G4 Δ(%) TLD	-3.5	3.5	2.8	4.4	13.1	11.9	14.3	14.3	58.3	28.3	-3.1
TLD ID	34	35	36	37	38	39	40	41	42	43	44
Organ**	LF	LE	LE	LE	PE	PE	AE	AE	AE	RE	RE
I/O/E*	O	O	O	O	O	O	O	O	O	O	O
TLD Dose (Gy)	0.5	0.5	0.5	0.6	0.5	0.5	0.5	0.5	0.5	0.6	0.6
G1 Δ(%) TLD	50.9	9.9	11.7	12.4	-15.2	-9.9	-11.3	-12.4	-7.7	8.0	11.4
G2 Δ(%) TLD	22.1	12.4	12.8	15.4	-39.3	-39.3	-38.8	-42.3	-37.7	18.3	20.7
G4 Δ(%) TLD	20.6	16.3	16.6	20.3	-12.1	-7.1	-8.1	-8.8	-8.5	20.3	22.4
											19.1

Organs** = R (Rectum), B (Bladder), LF (Left Femur), RF (Right Femur), AE (Anterior Extremities), LE (Left Extremities), RE (Right Extremities), PE (Posterior Extremities), P (Prostate).

I/E/O* I = TLD present inside the exposed field; E = TLD present at the edge of the field; O = outside the exposed field.

0.8 Gy as the total absorbed dose in the prostate, the doses of the other ROIs were calculated. Table 3 tabulates the results per total absorbed dose in each organ.

The comparison between the total dose in the organ obtained from the experimental process using the TLDs and the data obtained from the participating MC groups showed a large percent variation. The G1 results show a maximum variation of 21% at right femur and minimum of -15% at posterior extremity. The TLDs placed at the posterior extremity were in the build-up region of the beam profile which is close to 1.4 up to 1.6 cm deep. This may lead to a large percentage variation as presented. It was also observed for the other groups results. Considering all four positions as, anterior and posterior extremities, the left and right extremities, all the variation were above 10%. These values were below 10% only in 6 cases. Even though, these results are within the expected by the groups, the difficulties in identifying the exact position of the isocenter on the MC simulations was the main issue for the MC groups.

The G2 results percentage variation were between -40% and 13%. The maximum variation values were on the anterior extremity and right femur. The G3 results showed variation values between -11% up to 17%, also having maximum variation value on the right femur. Group 4 obtained variation around -10.0% up to 19.0% and with a large variation at the right extremity and right femur position. G2 group found the highest variation compared to the TLDs considering the total dose in the organs.

Dose estimates in the organs were obtained from the calculated absorbed dose in each TLD located in the respective organs. For this, it was assumed that the total absorbed dose within the TLDs located in a organ is representative of the absorbed dose in this organ. This assumption assumes that the dose is homogenous throughout the organ volume. The larger the organ volume less true this assumption becomes. The number of TLDs in a organ, as well as their locations in organ volume are also factors that may affect the validity of the above assumption. It should therefore be noted that depending on the validity of the assumption assumed, the TLD values may or may not represent the

dose in the organs. One way to solve this question would be to simulate this case using a segmented anthropomorphic phantom (mathematical or voxel) and estimate the doses in the respective organs. Lee et al. (2015), developed methods to reconstruct organ doses for radiotherapy patients by using a series of computational human phantoms coupled with a commercial treatment planning system (TPS) and a radiotherapy-dedicated Monte Carlo transport code. They used Analytical Anisotropic Algorithm (AAA), the dose calculation algorithm employed on Eclipse™ (Varian Medical System, Palo Alto, CA) TPS, and the X-ray Voxel Monte Carlo (XVMC) code (Fippel, 1999). Their results for organ average doses matched within 7%, whereas maximum and minimum point doses differed up to 45%. Thus, there are few points to be discussed. The MC code used was not the same for the different MCMC groups of researchers and, instead of hybrid voxel computational human phantoms, the voxel phantom based on Alderson-Rando Pelvic Phantom images was used. The xIO TPS used in this work is based on superposition algorithm. Furthermore, Lee et al. (2015) exported the organ contours from other code and this allowed them to have dose in a volumetric region. In this intercomparison exercise point doses were obtained. Point doses are the calculated doses of the TLDs placed in the phantom reference points which represents the organ. This allows to compare the absorbed dose from TLDs to the values obtained using the different MC codes. It was observed large variations between punctual doses as reported by Lee et al. (2015). Nevertheless, to our knowledge, there is no publication in the literature considering TLD dose measurements in physical pelvis phantom and MC simulations. Hosseini Pooya et al., 2014 (Pooya and Orouji, 2014) reported that it will be admissible to have such variations when simulation results are compared to the TLD measurements if we consider the directional dependence, energy dependence, fading, the dependence on ambient temperature and humidity, and the electronic characteristics of the TLD-reader system.

The second type of analysis was then performed by considering the TLD doses individually with a purpose to understand the reason behind such large variations. Table 4 shows the results obtained when TLD

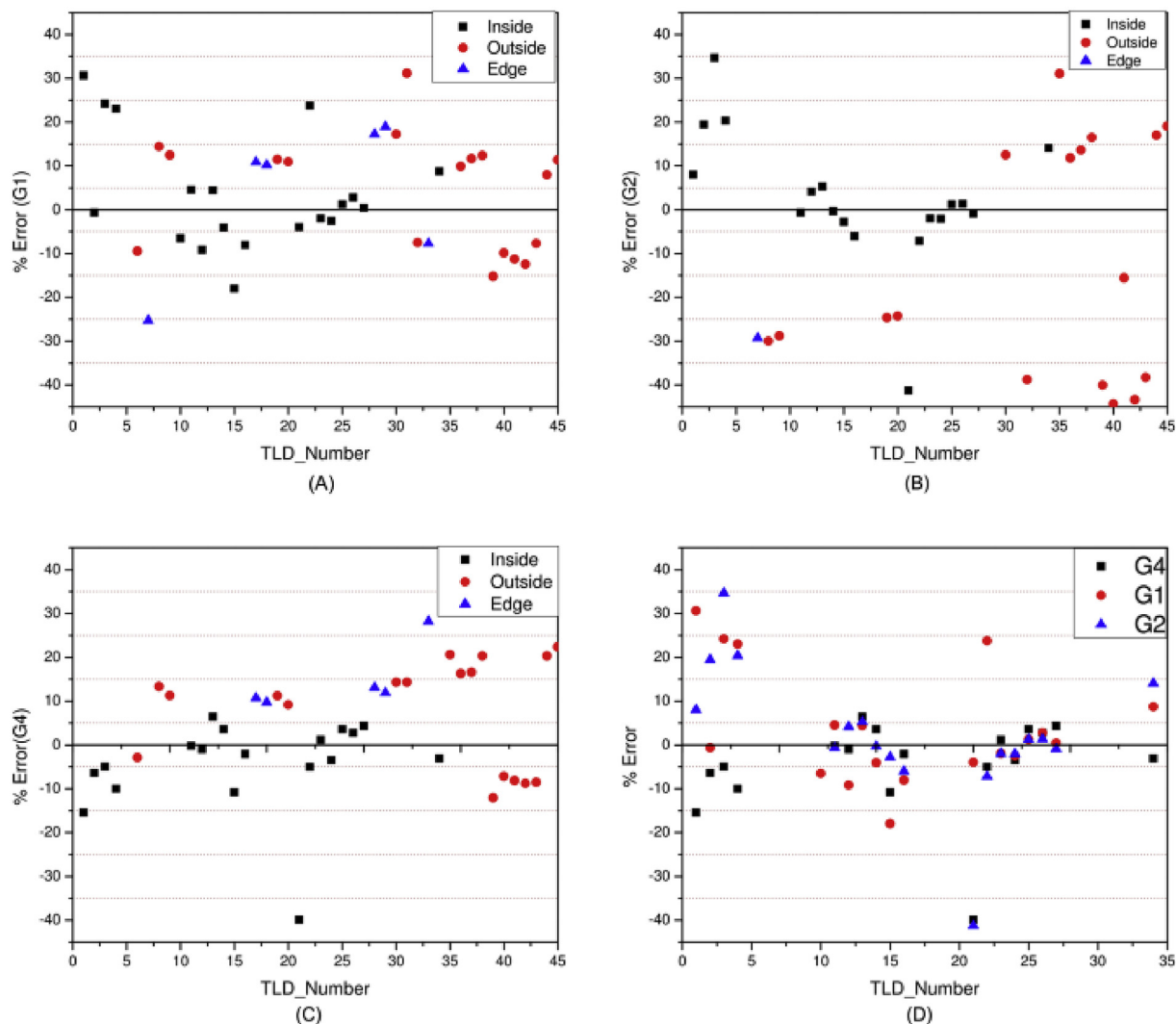


Fig. 4. (A) Representation of the uncertainty obtained by G1 for TLDs inside, outside or at the edge of the radiation field. Similarly, (B) representation of the uncertainties obtained by G2 and (C) for uncertainties obtained by G4, (D) representation of the uncertainties obtained by G1, G2, and G3 for the TLDs within the radiation field.

doses were analyzed individually. Unfortunately, due to the limitation of time Group 3 (EGS++) was not able to participate in this analysis. This table also shows the TLDs positions, whether they were placed inside, outside or at the edge of the exposed field (I/E/O).

Table 4 presents the doses obtained for each of the 45 TLDs, taking into account their positions within the radiation field. It can be observed that largest variations between the TLD measurements and MC calculations were obtained for the TLDs that were present on the edges or outside the radiation field. Fig. 4D shows the percentage variations obtained by G1, G2, and G4 for the TLDs within the radiation field with respect to the measurements. Fig. 4A depicts the variations obtained by G1 for TLDs inside, outside or at the edge of the radiation field. Similarly, Fig. 4B for G2, Fig. 4C for G4. G1 observed variation ranging from -25.3% to 51% , whereas for G2 ranging between -62% and 42% and for G4 between -75% and 58% with respect to the TLD measurements. If TLDs are considered according to their location G1, G2 and G4 reported largest variations for rectum, right femoral heads and left femoral heads. In addition to that G2 and G4 also reported considerable variations for extremities: 42% – 22% (G2) and -12% to 22% (G4). These observations are in well agreement with the results reported in Table 3. This variation can be a result of absence of enough build up region as in the case of extremities, or the presence of TLDs at the edge or outside the radiation field. G4 reported widest range of variations

(-75% – 58%).

This large range of percentage deviation can be explained as G4 used ESAVE_GLOBAL, a variance reduction parameter. In this case, if the particle falls below this value then IREJCT_GLOBAL calculates the range of the electron. If this range is not large enough for electron to cross the next boundary then it is discarded and all its energy is deposited in the surrounding region. The parameter was set as 2 MeV. The Directional Bremsstrahlung Splitting (DBS) was used to remove the low energy particles out of region of interest. As stated above the largest variations were observed for the TLD positions that were either at the edge or outside the radiation field. In general, if we consider only the TLDs placed inside the radiation field all groups G1, G2 and G4 observed variation within -10% to 10% with respect to the experimental results. Some spread points above 10% variation were also observed. If we consider the beam profile outside the geometric limits of the beam, in this case $10 \times 10 \text{ cm}^2$, there is an area of penumbra which represents the side scatter from the field or/and both leakage and scatter from the collimator system, this may explain the variation on the results concern to the TLDs outside and at the edge of the beam. Moreover, it remains speculative the observed trend variation on the MC groups.

6. Conclusions

The Monte Carlo Modelling Expert Group (MCMEG) is a research network. A multigroup dosimetric intercomparison exercise for modelling and simulating a case of prostate radiation therapy (RT) protocol was addressed. This intercomparison was launched sourcing the dose distribution in the prostate target volume and in the neighboring organs. Similar treatment plans were generated using different Monte Carlo codes. The simulations were performed using the MCNPx, MCNP6, and EGSnrc (egs+ + and BEAMnrc/DOSXYZnrc) Monte Carlo codes. Absorbed dose measurements were achieved by using TLDs. A protocol with a pair of two parallel-opposed fields was planned and performed on Alderson-Rando Pelvic Phantom. The assessed organs at risk were the urinary bladder, rectum and right and left femur heads. The major measured parameters were dose in the target volume, mean doses and standard deviation in the organs at risk, and dose volumes data. A comparison between the simulated results and the experimental values found on the TLDs were done. A large dose variation was observed when compared to the doses of the TLDs and this was explained by the difficulties in the modelling of the geometry and in setting all the parameters needed for the simulations as well as because of the systemic errors related with the TLD measurements. Even though, the exercise has been a great opportunity for the MC groups to learn and share the main difficulties found during the modelling and the analysis of the results. Concern to the large variation found, the MCMEG team consider that this was expected for the level of complexity of the exercise and this need to be study by the MC groups.

Acknowledgements

The following Brazilian institutions support this research project: Coordination for the Capacitation of Graduated Personnel (CAPES) and The authors also thank the Laboratório de Metrologia de Nêutrons of the Instituto de Radioproteção e Dosimetria (IRD/CNEN) for consenting the use of high-performance cluster for the computational calculations and the members of the MCMEG. Anyone doing modelling and simulation using MC are welcome to join this group. The MCMEG group website can be found at: [Monte_Carlo_Modelling_Expert_Group – groups.google.com](http://Monte_Carlo_Modelling_Expert_Group_groups.google.com).

References

- Abushab, K.M., Alajerami, Y.S., Alagha, S., Hashim, S., 2017. Thermoluminescence energy response of copper and magnesium oxide doped lithium potassium borate using a Monte Carlo N-particle code simulation. *Int. J. Med. Phys. Clin. Eng. Radiat. Oncol.* 6 (03), 304.
- Bouchard, H., Seuntjens, J., 2004. Ionization chamber-based reference dosimetry of intensity modulated radiation beams. *Med. Phys.* 31 (9), 2454–2465.
- Budanec, M., Knežević, Ž., Bokulić, T., Mrčela, I., Vrtar, M., Vekić, B., Kusić, Z., 2008. Comparison of doses calculated by the Monte Carlo method and measured by LiF TLD in the buildup region for a 60Co photon beam. *Appl. Radiat. Isot.* 66 (12), 1925–1929.
- Castelo e Silva, L.A., Mendes, B.M., Paixão, L., Gonçalves, B.R., Santos, D.M.M., Vieira, M.V., Fonseca, T.C.F., 2016. Intercomparação Computacional do Modelo Matemático de um Acelerador Clínico LINAC 6 MV Utilizando dois Códigos de Monte Carlo Diferentes: mcnp6 e EGSnrc. *Braz. J. Radiat. Sci.* 4 (2), 1–18.
- Chen, R., Leung, P.L., 2001. Nonlinear dose dependence and dose-rate dependence of optically stimulated luminescence and thermoluminescence. *Radiat. Meas.* 33 (5), 475–481.
- Fippel, M., 1999. Fast Monte Carlo dose calculation for photon beams based on the VMC electron algorithm. *Med. Phys.* 26 (8), 1466–1475.
- Fonseca, T.C.F., Campos, T.P.R., 2016. SOFT-RT: software for IMRT simulations based on MCNPx code. *Appl. Radiat. Isot.* 117, 111–117.
- Fonseca, T.C.F., Mendes, B.M., Lacerda, M.A.D.S., Silva, L.A.C., Paixão, L., Bastos, F.M., Junior, J.P.R., 2017. MCMEG: Simulations of Both PDD and TPR for 6MV LINAC Photon Beam Using Different MC Codes. 10.1016.
- Gardner, E.A., Sumanaweera, T.S., Blanck, O., Iwamura, A.K., Steel, J.P., Dieterich, S., Maguire, P., 2012. In vivo dose measurement using TLDs and MOSFET dosimeters for cardiac radiosurgery. *J. Appl. Clin. Med. Phys.* 13 (3), 190–203.
- Goorley, T., James, M., Booth, T., Brown, F., Bull, J., Cox, L.J., Durkee, J., Elson, J., Fensin, M., Forster, R.A., Hendricks, J., Hughes, H.G., Johns, R., Kiedrowski, B., Martz, R., Mashnik, S., McKinney, G., Pelowitz, D., Prael, R., Sweezy, J., Waters, L., Wilcox, T., Zukaitis, T., 2012. Initial MCNP6 release overview. *Radiat. Transp. Prot.* 180 (3), 298–315.
- Kawrakow, I., 2000. Accurate condensed history Monte Carlo simulation of electron transport. I. EGSnrc, the new EGS4 version. *Med. Phys.* 27 (3), 485–498.
- Kawrakow, I., Rogers, D.W.O., Walters, B.R.B., 2004. Large efficiency improvements in BEAMnrc using directional bremsstrahlung splitting: directional bremsstrahlung splitting. *Med. Phys.* 31 (10), 2883–2898.
- Kawrakow, I., Mainegra-Hing, E., Tessier, F., Walters, B.R.B., 2009. The EGSnrc C++ Class Library. *NRC Report PIRS-898 (rev A)*.
- Knöös, T., Wieslander, E., Cozzi, L., Brink, C., Fogliata, A., Albers, D., Lassen, S., 2006. Comparison of dose calculation algorithms for treatment planning in external photon beam therapy for clinical situations. *Phys. Med. Biol.* 51 (22), 5785.
- Lee, C., Jung, J.W., Pelletier, C., Pyakuryal, A., Lamart, S., Kim, J.O., Lee, C., 2015. Reconstruction of organ dose for external radiotherapy patients in retrospective epidemiologic studies. *Phys. Med. Biol.* 60 (6), 2309.
- Limited, B.S., 2014. BS ISO 28057:2014. Dosimetry with solid thermoluminescence detectors for photon and electron radiations in radiotherapy. In: *BSI Standards Limited 2014, Switzerland, ISO 28057:2014(E)*.
- Mainegra-Hing, E., Rogers, D.W.O., Tessier, F., Walters, B.R.B., 2017. The EGSnrc Code System: Monte Carlo Simulation of Electron and Photon Transport. *National Research Council Canada Technical Report PIRS-701*.
- MCMEG, 2018MCMEG, <https://groups.google.com/forum/#!forum/mcmeg>, Accessed date: 29 March 2018.
- Mendes, B.M., Almeida, I.G., Trindade, B.M., Campos, T.P.R., 2014. A female voxel phantom for radiopharmaceuticals internal dosimetry. In: *4th International Nuclear Chemistry Congress*, pp. 317–318.
- Montano-García, C., Gamba-de Buen, I., 2006. Measurements of the optical density and the thermoluminescent response of LiF: Mg, Ti exposed to high doses of 60Co gamma rays. *Radiat. Protect. Dosim.* 119 (1–4), 230–232.
- Paixão, L., Facure, A., Santos, A.M.M., Santos, A.M., Grynberg, S.E., 2012. Monte Carlo study of a new I-125 brachytherapy prototype seed with a ceramic radionuclide carrier and radiographic marker. *J. Appl. Clin. Med. Phys.* 13 (3), 74–82.
- Pelowitz, D.B., 2011. MCNPX USER'S MANUAL Version 2.7. 0-1A-CP-11-00438. Los Alamos National Laboratory.
- Pham, T.M., 2009. Simulation of the Transmitted Dose in an EPID Using a Monte Carlo Method. (Doctoral Dissertation).
- Pooya, S.H., Orouji, T., 2014. Evaluation of effective sources in uncertainty measurements of personal dosimetry by a Harshaw TLD system. *Journal of biomedical physics & engineering* 4 (2), 43.
- Rijken, J.D., 2014. Calibration of TLD700: LiF for Clinical Radiotherapy Beam Modalities and Verification of a High Dose Rate Brachytherapy Treatment Planning System. (Doctoral Dissertation).
- Rogers, D.W.O., 2006. Fifty years of Monte Carlo simulations for medical physics. *Phys. Med. Biol.* 51 (13), R287.
- Rogers, D.W.O., Walters, B., Kawrakow, I., 2009. BEAMnrc users manual. *Nrc Report Pirs 509, 12*.
- Ross, G.M., 1999. Induction of cell death by radiotherapy. *Endocr. Relat. Cancer* 6 (1), 41–44.
- Schiefer, H., Fogliata, A., Nicolini, G., Cozzi, L., Seelentag, W.W., Born, E., Vallet, V., 2010. The Swiss IMRT dosimetry intercomparison using a thorax phantom. *Med. Phys.* 37 (8), 4424–4431.
- Seemann, K.M., Luysberg, M., Révay, Z., Kudejova, P., Sanz, B., Cassinelli, N., Schmid, T.E., 2015. Magnetic heating properties and neutron activation of tungsten-oxide coated biocompatible FePt core-shell nanoparticles. *J. Control. Release* 197, 131–137.
- Seniwal, B., Fonseca, T.C., Singh, R., 2019. Monte-carlo modelling for evaluation of two different calculation algorithms. *Brazilian Journal of Radiation Sciences* 7 (1).
- Shen, V.K., Siderius, D.W., Krekelberg, W.P., Hatch, H.W., 2018. NIST Standard Reference Simulation Website, NIST Standard Reference Database Number 173. National Institute of Standards and Technology, Gaithersburg MD 20899.
- Tai, D.T., Son, N.D., Loan, T.T.H., Trang, N.T.H., 2017. June. Initial experiences of applying the jaws-only IMRT technique in dong nai general hospital, Vietnam. In: *International Conference on the Development of Biomedical Engineering in Vietnam*. Springer, Singapore, pp. 335–339.
- Walters, B.R.B.I., Kawrakow, I., Rogers, D.W.O., 2005. DOSXYZnrc users manual. *Nrc Report Pirs 794, 31*.
- Werner, C.J., 2017. MCNP Users Manual-Code Version 6.2. Los Alamos National Laboratory, Los Alamos.
- Werner, C.J., Bull, J.S., Solomon, C.J., Brown, F.B., McKinney, G.W., Rising, M.E., Zukaitis, A.J., 2018. *MCNP Version 6.2 Release Notes* (No. LA-UR-18-20808). Los Alamos National Lab.(LANL). Los Alamos, NM (United States).